ICMA 2021
1st International Conference on Micromachines and Applications
15–30 APRIL 2021 | ONLINE

Sensitivity Analysis of a Portable Wireless PCB-MEMS Permittivity Sensor Node for Non-Invasive Liquid Recognition

micromachines
MDPI

Javier Meléndez-Campos [1], Matias Vázquez-Piñón [1], and Sergio Camacho-León [1,*]

[1] Tecnologico de Monterrey, School of Engineering and Sciences, Ave. Eugenio Garza Sada 2501, Monterrey, N.L., México, 64849.

* Corresponding author: sergio.camacho@tec.mx

Tecnológico de Monterrey

Sensitivity Analysis of a Portable Wireless PCB-MEMS Permittivity Sensor Node for Non-Invasive Liquid Recognition

Graphical Abstract

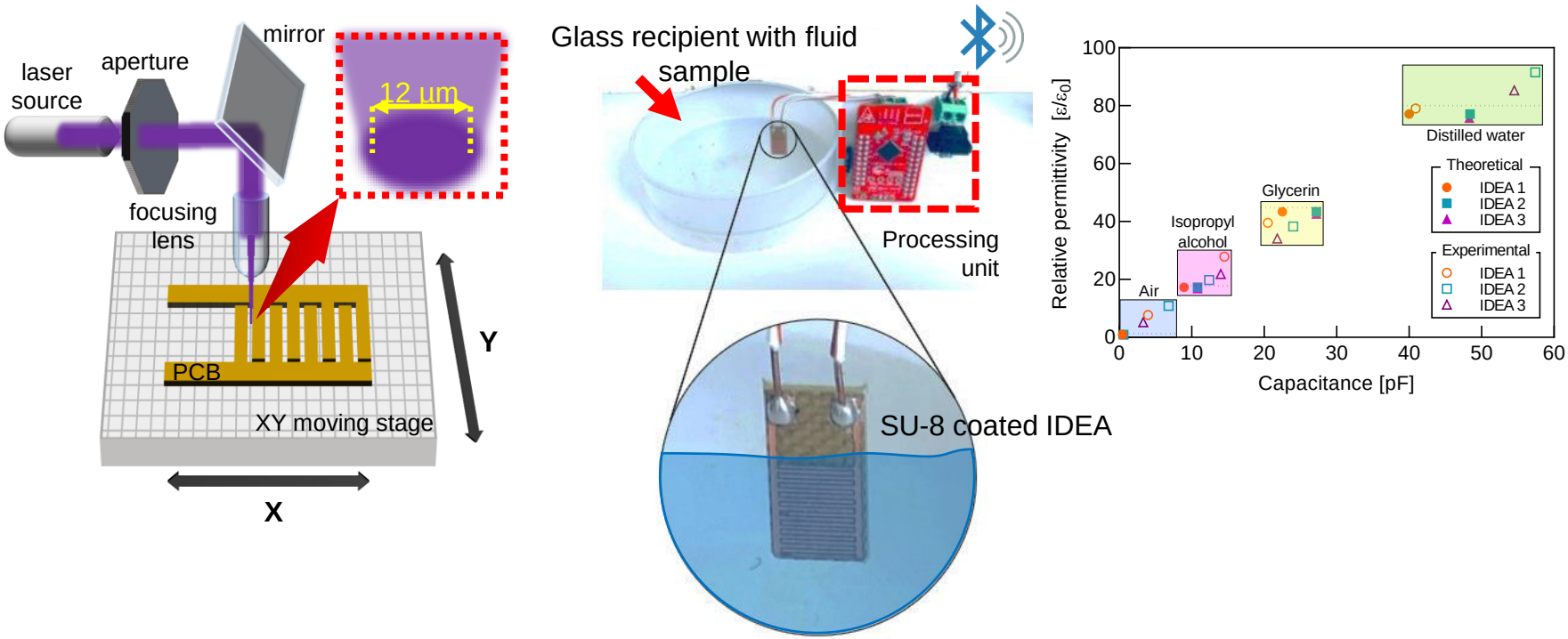

ICMA 2021

Abstract:

Dielectric characteristics are useful to determine crucial properties of liquids and to differentiate between liquid samples with similar physical characteristics. Liquid recognition has found applications in a broad variety of fields, including healthcare, food science, and quality inspection, among others. This work demonstrates the fabrication, instrumentation, and functionality of a portable wireless sensor node for permittivity measurement of liquids that require characterization and differentiation. The node incorporates an interdigitated microelectrode array as transducer, and a microcontroller unit with radio communication electronics for data processing and transmission, which enables a wide variety of stand-alone applications. A laser-ablation-based microfabrication technique is applied to fabricate the microelectromechanical systems (MEMS) transducer on a printed circuit board (PCB) substrate. The surface of the transducer is covered with a thin layer of SU-8 polymer by spin coating, which prevents from direct contact between the Cu electrodes and the liquid sample. This helps to enhance durability, avoid electrode corrosion and contamination of the liquid sample, and to prevent undesirable electrochemical reactions to arise. The transducer's impedance was modeled as a Randles cell, having resistive and reactive components determined analytically using a square wave as stimuli, and a resistor as a current-to-voltage converter. To characterize the node sensitivity under different conditions, three different transducer designs were fabricated and tested for four different fluids—i.e., air, isopropanol, glycerin, and distilled water—achieving a sensitivity of 1.6965 +/- 0.2028 εr/pF. The use of laser ablation allowed the reduction of the transducer footprint while maintaining its sensitivity within an adequate value for the targeted applications.

Keywords: PCB-MEMS; Permittivity sensor; Liquid recognition

ICMA 2021

Introduction

- **Liquid recognition** has found applications in a broad variety of fields, including healthcare [1], food science [2], and quality inspection [3], among others.
- **Dielectric characteristics** are useful to determine crucial properties of liquids, and to differentiate between liquid samples with similar physical characteristics.
- The capabilities of sensors for liquid characterization have been studied before, using **interdigitated electrodes arrays (IDEA)**.
- Due to its **capacitive nature**, IDEAs are suitable for measuring dielectric changes across their electrode fingers.
- Even though the data generated by one sensor could gather enough information for some applications, the conjunction of several **sensors as a network allow to achieve granularity and heterogeneity** in the collected information.

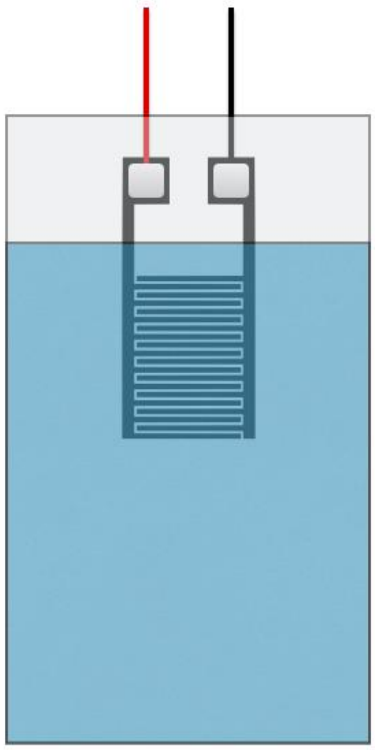

Interdigitated electrodes array (IDEA) immersed in a liquid sample

[1] T. Chen, D. Dubuc, M. Poupot, J. Fournié, and K. Grenier, "Accurate Nanoliter Liquid Characterization Up to 40 GHz for Biomedical Applications : Toward Noninvasive Living Cells Monitoring," vol. 60, no. 12, pp. 4171–4177, 2012.

[2] B. V. Oliinyk *et al.*, "Silicon-Based Optoelectronic Tongue for Label-Free and Nonspecific Recognition of Vegetable Oils," *ACS Omega*, vol. 5, no. 11, pp. 5638–5642, 2020, doi: 10.1021/acsomega.9b03196.

[3] X. Jiang *et al.*, "Rapid Liquid Recognition and Quality Inspection with Graphene Test Papers," *Glob. Challenges*, vol. 1, no. 6, p. 1700037, 2017, doi: 10.1002/gch2.201700037.

Towards an Internet of micro-Things

- **Goal:** To integrate sensing, processing, storage and communication capabilities into a small form factor device [4].

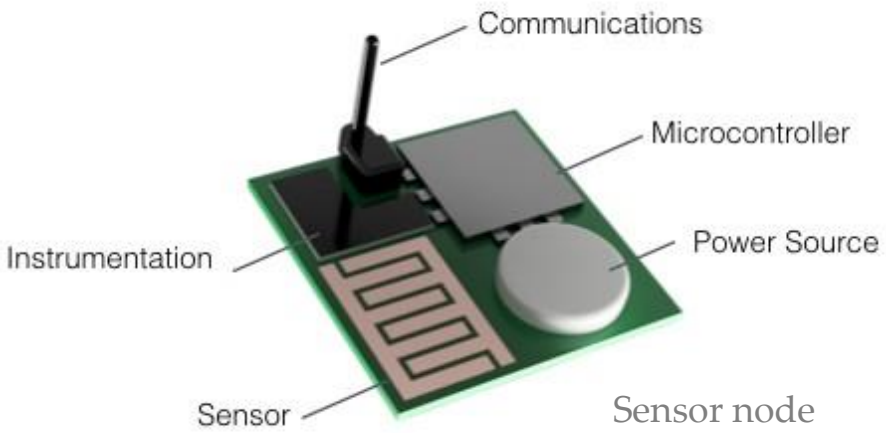

- **Micro-Electro-Mechanical Systems (MEMS)** have allowed the development of miniature (1 μm - 1 mm) sensors that open the possibility of large-scale deployment and scalability for **Wireless Sensor Network (WSN)**.
- However, the **cost-effectiveness** of **Si-based MEMS micromachining** [5,6] is only achieved at **high production volumes**.

[4] ITU, "ITU Internet Reports. The Internet of Things," 2005.
[5] F. A. Harraz, "Porous silicon chemical sensors and biosensors : A review," Sensors Actuators B. Chem., vol. 202, pp. 897–912, 2014, doi: 10.1016/j.snb.2014.06.048.
[6] C. Roychaudhuri, "A review on porous silicon based electrochemical biosensors : Beyond surface area enhancement factor," Sensors Actuators B. Chem., vol. 210, pp. 310–323, 2015, doi: 10.1016/j.snb.2014.12.089.

PCB-MEMS

- As an alternative to Si at the prototyping stage, **PCB-MEMS** use regular **printed circuit boards (PCB)** as substrate and allows maskless techniques, such as laser ablation and milling, to transfer previously-designed patterns to the PCB in a faster development cycle, achieving a resolution as low as 50 μm [7, 8].
- PCB fabrication techniques have been used previously in non-invasive liquid recognition applications using IDEAs, demonstrating the feasibility of this process in the field of liquid sensing [9].
- In this work, the sensing node incorporates a laser-ablated interdigitated microelectrode array as **transducer**, and a **microcontroller unit** with **radio communication electronics** for **data processing and transmission**, which enables a wide variety of stand-alone applications.

[7] M. Contreras-Saenz, C. Hassard, R. Vargas-Chacon, J. L. Gordillo, and S. Camacho-Leon, "Maskless fabrication of a microfluidic device with interdigitated electrodes on PCB using laser ablation," Microfluid. BioMEMS, Med. Microsystems XIV, vol. 9705, p. 97050N, 2016, doi: 10.1117/12.2222961.

[8] M. Contreras-Saenz, R. M. Vargas-Chacon, J. M. Rodriguez-Delgado, and S. Camacho-Leon, "PCB-MEMS: Fabrication of Active Microfluidic Devices by Laser Ablation," in Laser Ablation: Advances in Research and Applications, Nova Science Publishers: Hauppage, 2017.

[9] A. Vuković Rukavina, "Non-invasive liquid recognition based on interdigital capacitor," Sensors Actuators, A Phys., vol. 228, pp. 145–150, 2015, doi: 10.1016/j.sna.2015.03.019.

Materials and Methods: Transducer

- The IDEA transducer described in this paper is considered as **symmetric coplanar**.
- **Geometric variables:** finger count (***N***), gap between adjacent fingers (***g***), finger width (***w***), and finger overlapping length (***l***).
- **Equivalent circuit:** the medium resistance in series with the electrode's resistance (Rsp), a double layer capacitance due to the charge transfer process (Cp) at the electrode-electrolyte interface, and a charge transfer or polarization resistance (Rp) [10].

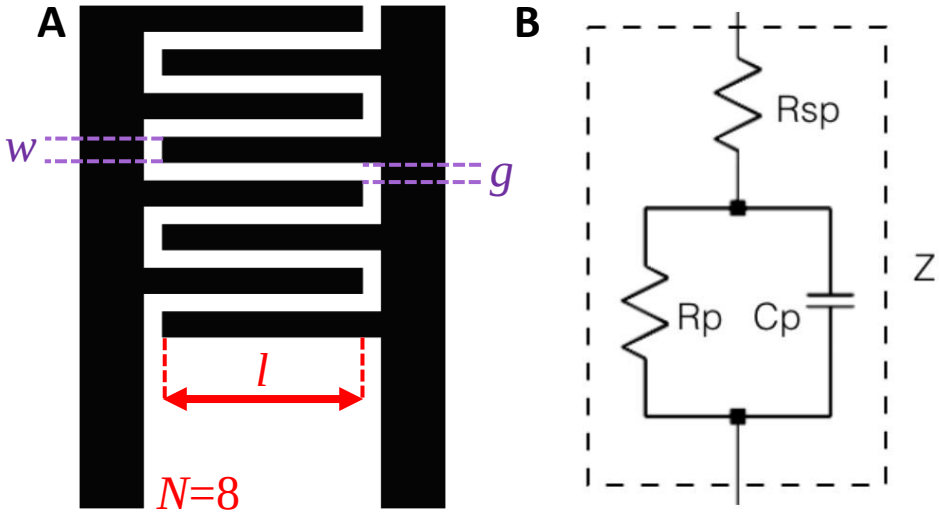

Geometric variables Equivalent circuit: Randles cell

g a ***w*** strongly depend on the resolution of the microfabrication process

[10] J. E. B. Randles, "Kinetics of rapid electrode reactions," Faraday Discuss., 1947, doi: 10.1039/DF9470100011.

Capacitance modeling

- The **total capacitance** of an IDEA is determined by the sum of all parallel plates capacitors in it as [11, 12]

$$\boldsymbol{C_p = C_l(N-1)l}$$

where

The double layer capacitance between the metal electrodes and the liquid sample is $C_l = \frac{\varepsilon_0 \varepsilon_r}{2} \frac{\mathrm{K}\sqrt{1-q}}{\mathrm{K}(q)}$

The vacuum permittivity is $\varepsilon_0 = 8.854x10^{-12}\ \mathrm{F \cdot m^{-1}}$

The dielectric constant of the liquid sample is ε_r.

The complete elliptic integral of the first kind is $\mathrm{K}(q) = \int_{t=0}^{1} \frac{dt}{\sqrt{(1-t^2)(1-q^2t^2)}}$

Here, q is a geometric term that depends on w and g.

For a parallel plate capacitor $q = \frac{g}{g+w}$

For multiple plates in parallel $q = \cos\left(\frac{\pi}{2}\frac{w}{g+w}\right)$

- The **total footprint area** can be approximated as $\boldsymbol{A_t = N \times l(w+g)}$.

[11] Javier Melendez-Campos, "Fabrication of an integrated PCB-MEMS dielectric sensor node for liquid characterization"; M.Sc. Thesis, Tecnologico de Monterrey; Mexico, May. 2017.

[12] W. Olthuis, W. Streekstra, and P. Bergveld, "Theoretical and experimental determination of cell constants of planar-interdigitated electrolyte conductivity sensors," Sensors Actuators B. Chem., 1995, doi: 10.1016/0925-4005(95)85053-8.

Sensitivity analysis

- $\frac{\partial C_p}{\partial \varepsilon_r}$ with respect to the footprint area of the IDEA.

In this analysis $\boldsymbol{\varepsilon_r}$ = 80 (distilled water), $\boldsymbol{g}$ = 100 μm, $\boldsymbol{l}$ = 4.3 mm, $\boldsymbol{w}$ = 250 μm, and the **number of fingers was varied** from $\boldsymbol{N}$ = 4 to 42 by increments of 2.

The linear sensitivity increase with respect to the footprint area of the transducer is due to the **stepped effective surface increments of the sensing area** due to the **adding of electrode pairs**.

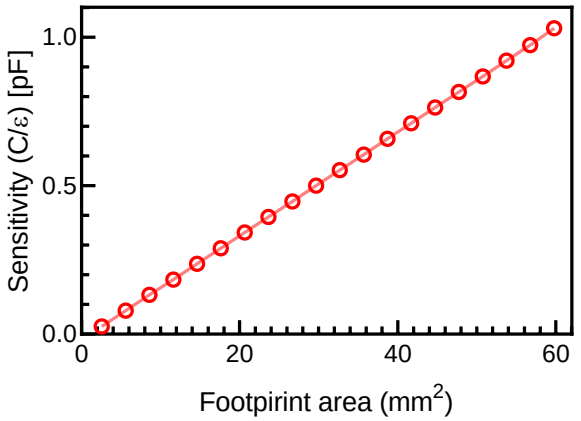

- $\frac{\partial C_p}{\partial \varepsilon_r}$ with respect to the gap between adjacent fingers of the IDEA.

In this analysis $\boldsymbol{\varepsilon_r}$ = 80 (distilled water), $\boldsymbol{N}$ = 10, $\boldsymbol{l}$ = 4.3 mm, $\boldsymbol{w}$ = 250 μm, and the **gap was varied*** from $\boldsymbol{g}$ = 10 μm to 200 μm by increments of 10 μm.

A decrease in the gap between the fingers considerably increases the sensitivity of the electrodes, without significantly increasing the footprint area of the transducer.

*strongly depend on the resolution of the microfabrication process

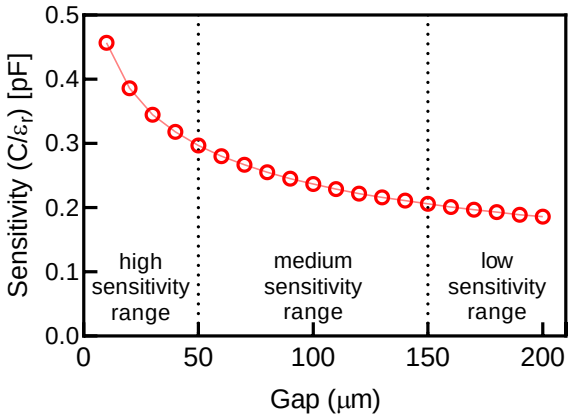

ICMA 2021

Laser ablation process for PCB-MEMS fabrication

- Laser ablation is a cost-effective technique that allows the fabrication of **well-defined structures** and **small gaps** (Slide 23: Supplementary Material) in a **small footprint area**.
- This technique **overcomes the lack of precision** of traditional **PCB machining** techniques, while **reducing the fabrication time and cost**, compared to **photolithography**, at the **prototyping stage**.

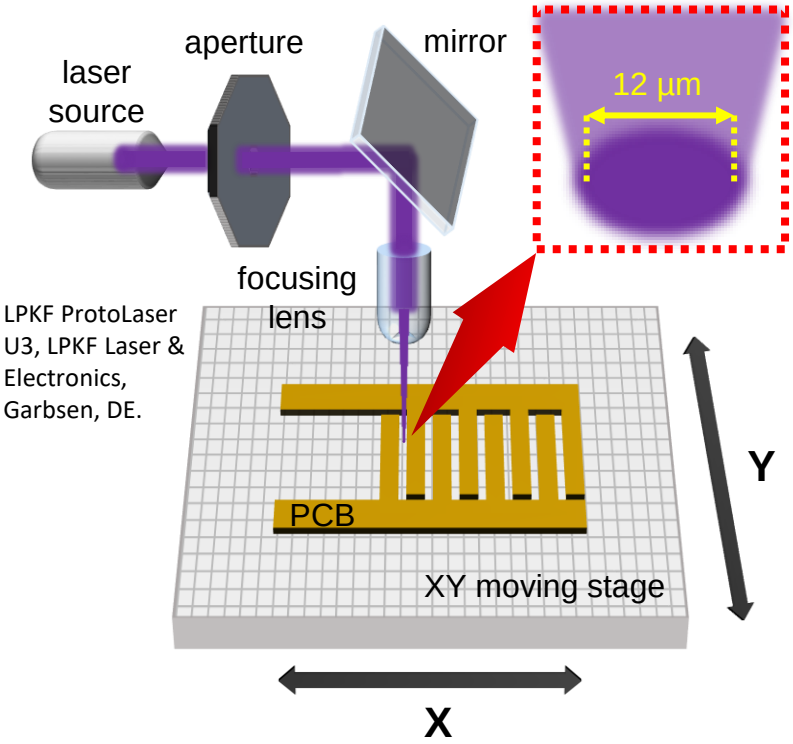

Optical setup

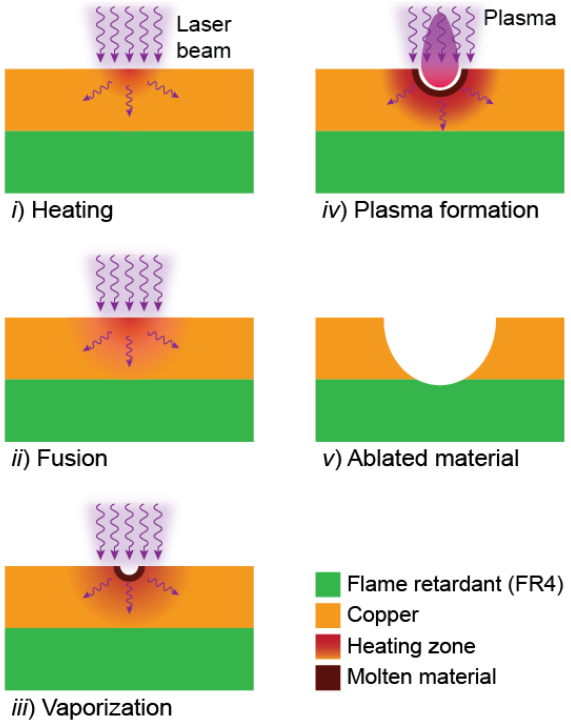

Steps of material removal by laser irradiation

ICMA 2021

Laser ablation process for PCB-MEMS fabrication

- **Three different IDEA designs** were fabricated in order to compare the effect of different effective footprint areas on the resulting capacitance Cp.
- The surface of the transducer is covered with a **thin layer of SU-8 polymer** by **spin coating**, which prevents from direct contact between the Cu electrodes and the liquid sample. This helps to enhance durability, **avoid electrode corrosion and contamination of the liquid sample**, and to **prevent undesirable electrochemical reactions** to arise.

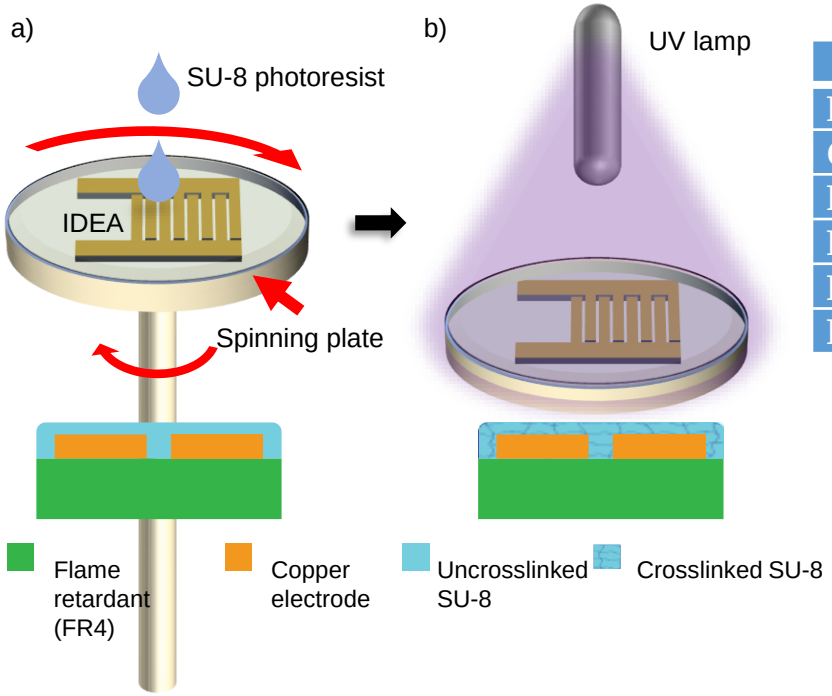

Spin-coating UV exposure

Geometric features of the three fabricated IDEAs

Geometric feature	IDEA 1	IDEA 2	IDEA 3
Finger width (w)	250 µm	250 µm	250 µm
Gap between fingers (g)	100 µm	100 µm	100 µm
Finger length (l)	4.3 mm	4.3 mm	5.2 mm
Finger height (h)	18 µm	18 µm	18 µm
Finger count (N)	20	24	20
Footprint area (A)	30.1 mm^2	36.1 mm^2	36.4 mm^2

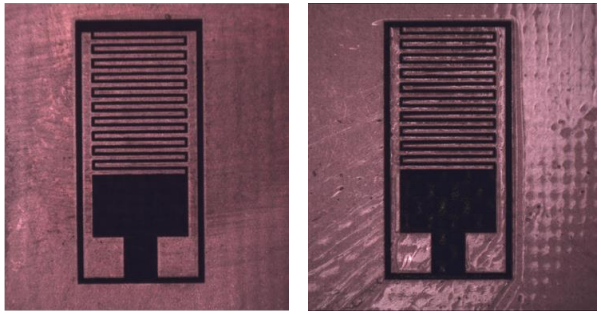

IDEA before and after Su-8 deposition

ICMA 2021

Instrumentation

- A resistor Rr working as a Current-to-Voltage-Converter (CTVC) is connected in series to the impedance transducer modeled as a Randles cell.
- The circuit is stimulated by a square wave pulse with a period Tp and 50% duty cycle, generated by the microcontroller.
- Rr = 1 MΩ and Tp = 1 ms are proposed to achieve capacitances in order of pF.
- The principle of operation is a voltage divider, in which the value of Rsp, Rp, Cp can be analytically deduced based on 3 output voltage measurements at different sampling times, as in [13].
- The low-cost 32-bit, 48 MHz **CY8C424LQI Programmable system-on-chip (PSoC)** (Cypress Semiconductors Corporation, San Jose, CA, USA) was implemented as the microcontroller unit (MCU) for the designed sensor node.

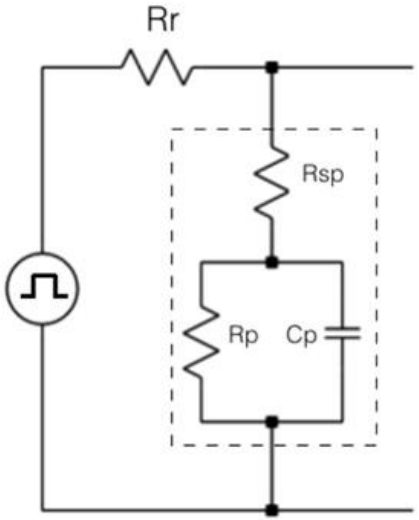

[13] Z. Czaja, "A microcontroller system for measurement of three independent components in impedance sensors using a single square pulse," Sensors Actuators, A Phys., vol. 173, no. 1, pp. 284–292, 2012, doi: 10.1016/j.sna.2011.10.018.

Experimental Setup

- In order to **validate the performance** of the sensor node, **four different fluid samples** were characterized—i.e. air (εr = 1), isopropyl alcohol (εr = 17.9), glycerin (εr = 45), and distilled water (εr = 80).
- These fluid samples were chosen due to their widespread dielectric constants.
- Different 60 ml glass recipients were used to test the transducer performance for each fluid sample and all the tests were carried out at **room temperature**.
- Measurements were taken during **2 min** and then the transducer was removed from the fluid sample.
- All the transducers were cleaned using isopropanol and distilled water after each measurement.

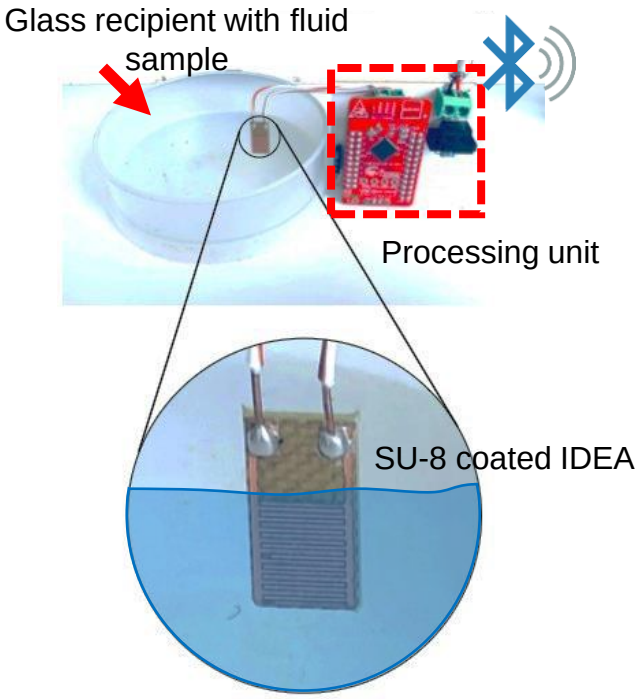

Experimental setup

- **Bluetooth Low Energy (BLE)** was used to report transducer changes to external observers. This protocol allowed a battery efficient transmission while sending data only when needed. The protocol overhead was short hence the size of package is maintained as small as possible.

Results: Transducer response

- Transducers response to input pulse for different testing fluids: a) IDEA 1, b) IDEA 2, and c) IDEA 3.
- To verify reproducibility of results, two different devices with the same feature sizes were used for each testing liquid, and the plots represent the mean of the two responses for each device and test fluid.

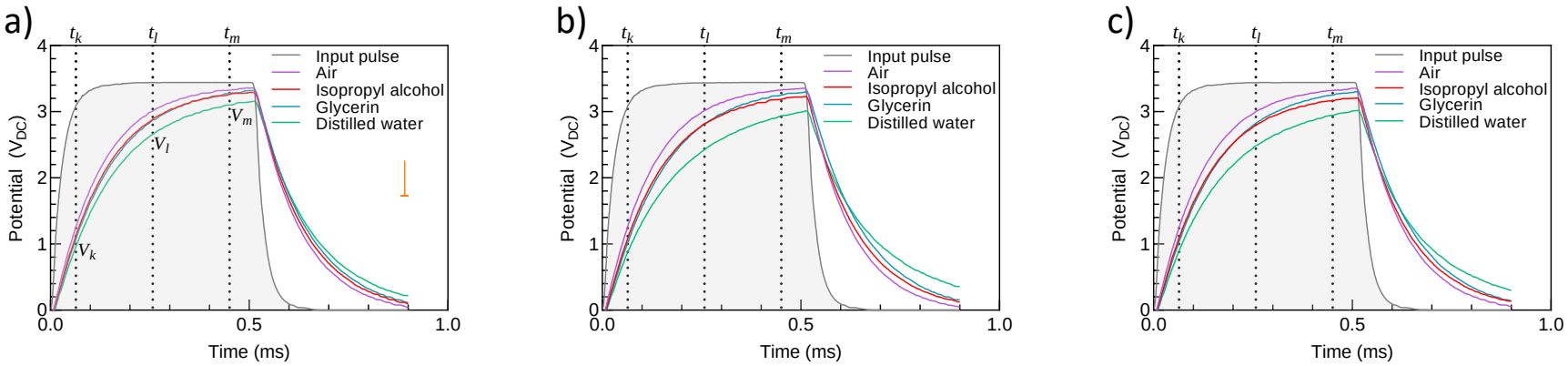

Pulse amplitude = 3.45 V
Pulse frequency = 1 kHz
Pulse duty cycle = 50%

$$t_k = T/8$$
$$t_l = 4T/8$$
$$t_m = 7T/8$$

ICMA 2021

Discussion: Transducer response

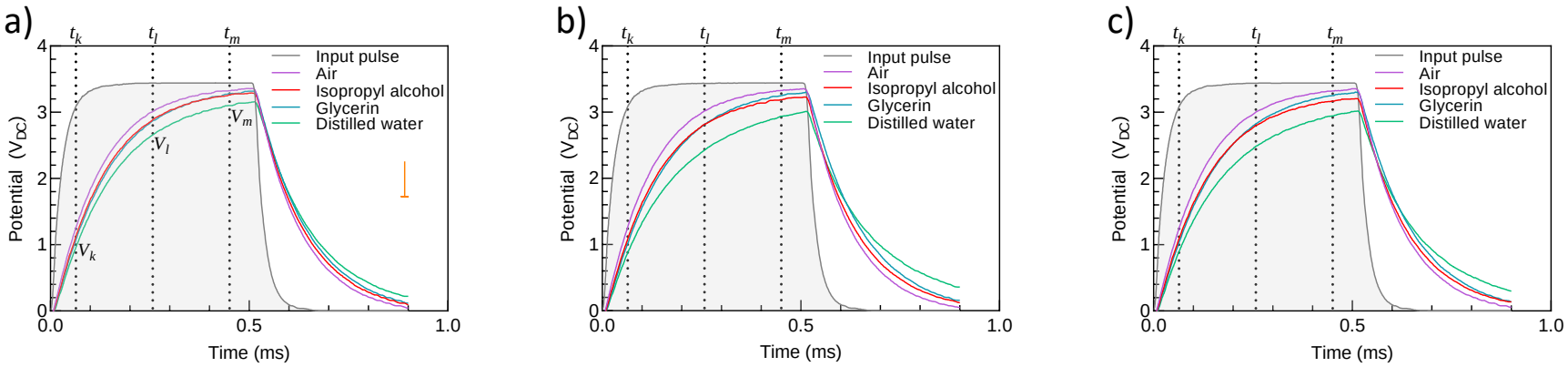

- The transducer response to air is particularly similar in all three cases.

This is because air—with the smallest permittivity value—can be considered as open circuit from the transducer point of view—i.e., infinite impedance, thus no current flowing thought it—and, in consequence, the transducer reaches the maximum output voltage possible (~3.3 V).

- Interestingly, our measurements show that a transition occurs on the measurements between isopropyl alcohol and glycerin, as the charging cycle evolves.

At tk, measurements for IDEA 1 averaged 1.1 V, 2.84 V and 3.24 V for isopropyl alcohol, and 1.04 V, 2.84 V and 3.28 V for glycerin. As expected, for tk, isopropyl alcohol shows a higher potential than glycerin—by a difference of **0.06 V**—due to a lower permittivity value. However, at tl, this difference is canceled out, to finally reverse at tm by **0.44 V**. This effect is consistently observed for IDEAs 2 and 3 with small variations on the potential different at the three sampling times.

- Finally, measurements for distilled water show the lowest values for all three transductors.

ICMA 2021

Results & Discussion: Capacitance

- Determined from theoretical calculations* (Slide 8: Capacitance modeling) and measurements**.

* For simplification purposes, the SU-8 layer covering the structures is not considered in these calculations.

** A linearity analysis based on experimental results shows that the transducers presented an average offset of 133.3 pF.

This is a system constant that considers the **output capacitance of the wave generator or the microcontroller**. The system constant was measured by running the algorithm without the transducer connected, in an early calibration stage.

Transducer	Air		Isopropyl alcohol		Glycerin		Distilled water	
	Theoretical	Experimental	Theoretical	Experimental	Theoretical	Experimental	Theoretical	Experimental
IDEA 1	0.49 pF	3.98 pF	8.94 pF	14.5 pF	22.48 pF	20.5 pF	39.97 pF	40.9 pF
IDEA 2	0.60 pF	6.82 pF	10.82 pF	12.4 pF	27.22 pF	24.0 pF	48.39 pF	57.4 pF
IDEA 3	0.60 pF	3.32 pF	10.81 pF	14.0 pF	27.19 pF	21.8 pF	48.34 pF	54.5 pF

- On average, IDEA 2 showed the smallest RPE (14%); meaning that IDEA 2 follows the closest to the ideal behavior of a theoretical transducer, which is consistent since it is the one with the highest finger count number of fingers $N = 24$.

Results: Relative permittivity estimations

- Relative permittivity can be calculated from capacitance measurements and theoretical calculations (Slide 8: Capacitance modeling).

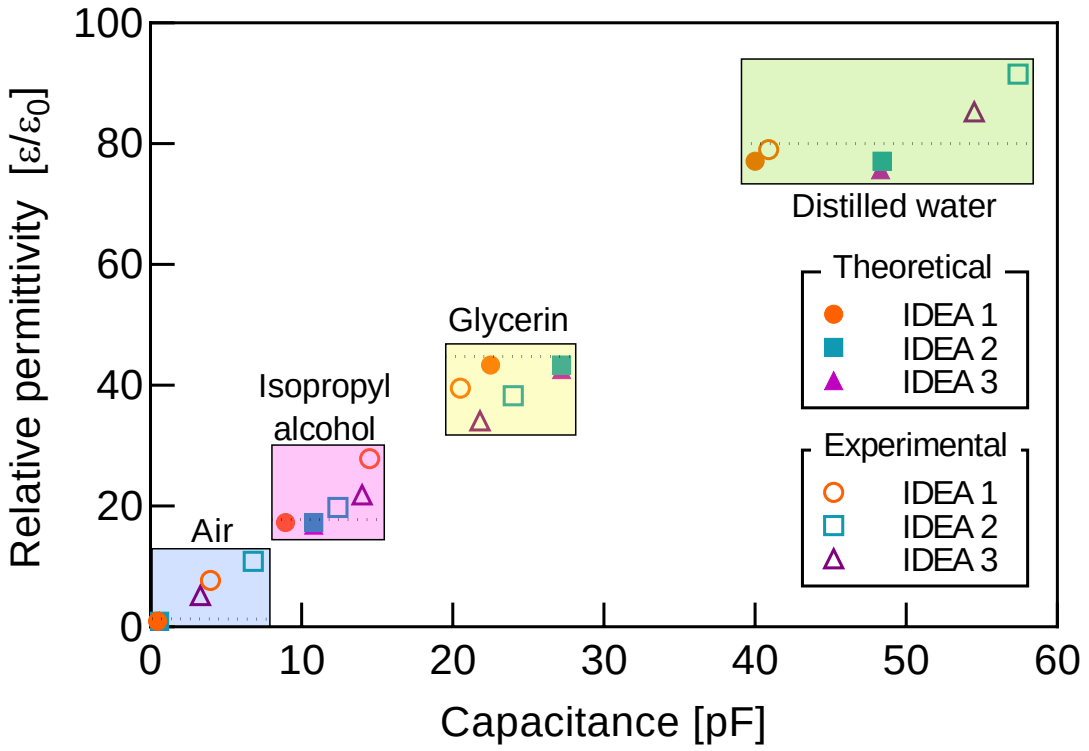

The dotted line indicates the standard value for each testing fluid.

Relative permittivity estimations from experimental capacitance measurements and theoretical calculations for the three IDEAs 1, 2 and 3

Discussion: Relative permittivity estimations

- As expected, permittivity estimations from theoretical capacitance values locate closer to the corresponding standard permittivity value of each testing fluid in almost all cases, while permittivity estimations from experimental measurements are found relatively farther from this standard value.

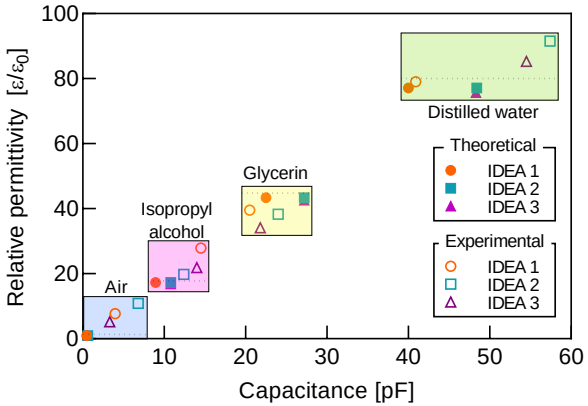

- However, for all four testing fluids, relative permittivities from both, theoretical and experimental inputs can be enclosed into a narrow range without overlapping, which suggests that for fluids with relative permittivities sufficiently spread, the low-cost fabrication process used in this work is suitable for the development of transducers with high enough differentiation rate.

- Furthermore, for IDEA 1, with the overall smallest RPE of all three transducers, the permittivity range could be narrowed even further, thus possibly reducing the permittivity difference among testing fluids.

ICMA 2021

Results & Discussion: Sensitivity

- Both, theoretical and experimental values confirm that the transducers with the highest footprint areas have the highest sensitivities.

Transducer	Footprint area, mm^2	Sensitivity, pF/ε_r		
		Theoretical	Experimental	RPE
IDEA 1	30.1	0.5186	0.5181	0.10%
IDEA 2	36.1	0.6274	0.6272	0.04%
IDEA 3	36.4	0.6382	0.6390	0.12%

- A least square fit allow to obtain the experimental regression line for the relative permittivity as

$$\varepsilon_r = \frac{\partial \varepsilon_r}{\partial C_p} C_p$$

where

$$\frac{\partial \varepsilon_r}{\partial C_p} \cong 1.6965 \pm 0.2028$$

C_p is in pF

Conclusions

- The use of a PCB-based IDEA fabricated by laser ablation allowed the reduction of the transducer footprint while maintaining its sensitivity within an adequate value for the targeted applications.
  - This technique overcame the lack of precision of traditional PCB manufacturing techniques—e.g. chemical etching—while reducing the fabrication time and cost, compared to photolithography, at the prototyping stage.

- The transducer consisted of interdigitated electrodes that fulfill the characteristics of sensitivity, portability, and scalability for mobile and non-invasive liquid recognition applications, where the dielectric constant must be differentiated.
  - The system incorporates a previously reported method to analytically determine three independent components of the impedance of a transducer.
  - However, for the first time, this method was implemented on the PSoC CY8C424LQI, which provides IoT functionality to the sensor node by adding not only on-chip signal processing and signal generation, but also Bluetooth Low Energy (BLE) communication capabilities. Hence the use of an external component was avoided and reduced to a microcontroller and its internal components.

Work in progress

- Quantification of the effect of the SU-8 layer on the transducer capacitance by means of finite element analysis in COMSOL.

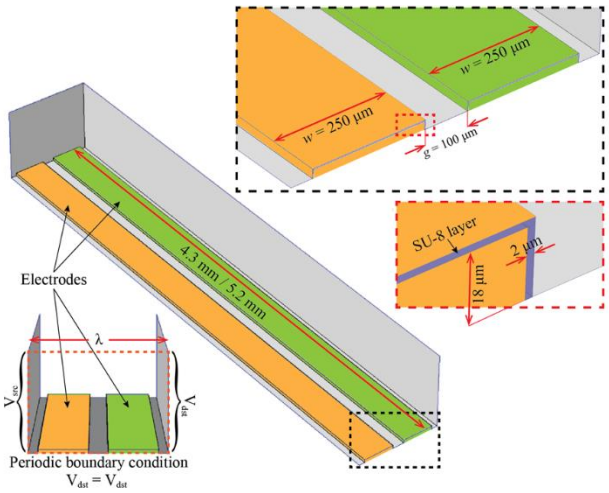

3D geometric definitions and established boundary conditions for the finite element analysis

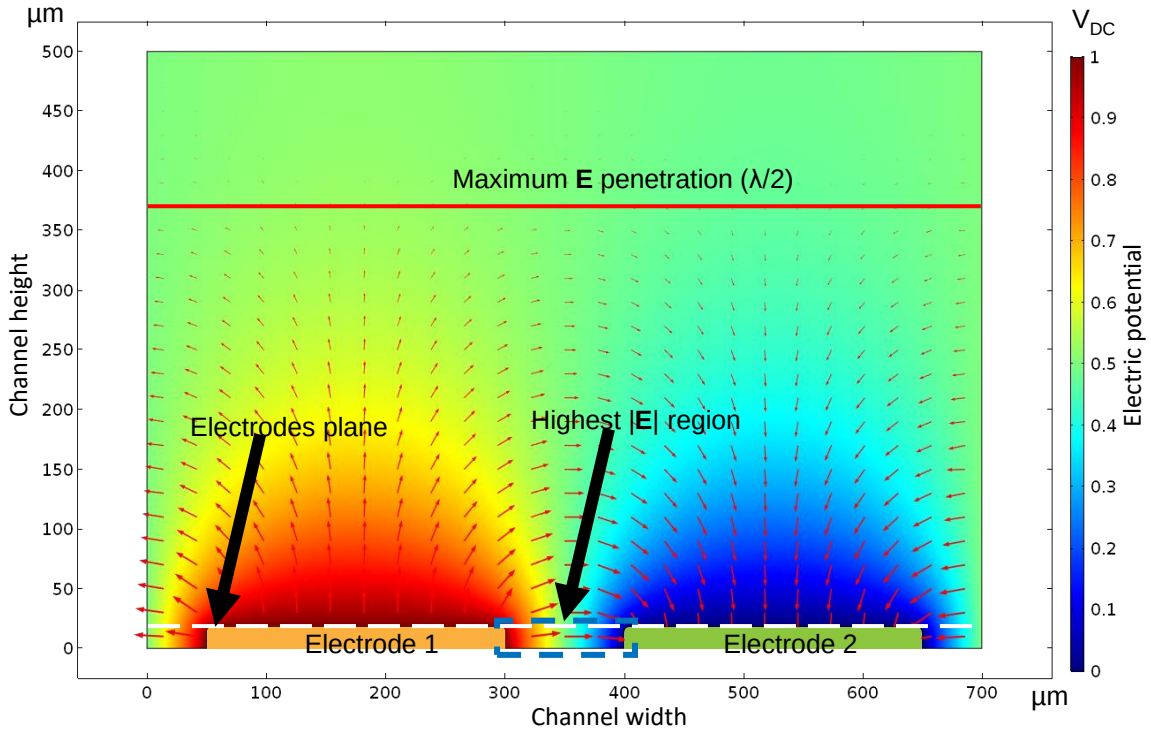

Electric potential and electric field distribution of a XY plane cut of the 3D model from the finite element analysis

ICMA 2021

Acknowledgments

The authors acknowledge financial support from the Tecnologico de Monterrey, through the research groups on Sensors and Devices, and on Robotics, as well as the National Robotics Laboratory of the Northeast and Central Area of Mexico at the School of Engineering and Sciences.

We thankfully acknowledge CONACyT (National Council for Science and Technology of Mexico) for the master's scholarship granted to JMC.

Supplementary Material

Geometrical characterization of the PCB-MEMS device fabricated from laser ablation

Geometric feature	CAD design	PCB device Mean (SD)	RPE
w [µm]	250	235.40 (9.7)	6.201%
l [mm]	4.3	4.36 (12.7)	1.578%
g [µm]	100	112.13 (9.5)	10.814%
A [mm^2]	30.1	30.4 (1.7)	0.878%

ICMA 2021